Deep learning for the design and characterization of high efficiency self-focusing grating

Tanchao Pu[1,2,3], Fulin Cao[1,2], Ziwei Liu[1,2], and Changqing Xie[1,2*]

[1]*Key Laboratory of Microelectronic Devices & Integrated Technology, Institute of Microelectronics of Chinese Academy of Sciences, Beijing 100029, China*

[2]*University of Chinese Academy of Sciences, Beijing 101408, China*

[3]*Optoelectronics Research Centre and Centre for Photonic Metamaterials, University of Southampton, Southampton SO17 1BJ, UK*

*xiechangqing@ime.ac.cn

Abstract: We demonstrate that the deep learning algorithm can considerably simplify the design and characterization of high efficient self-focusing varied line-spaced gratings. Our neural network is implemented with a recovery rate of up to 94% for the transmission function parameters. With numerical simulations, and optical experiments, we show that the self-focusing varied line-spaced gratings designed in such a way are endowed with enhanced functionalities, such as the intensity of first-order diffraction peak being enhanced with around a factor of 30 compared with the incident intensity, and a high ratio (about 60) between the peak intensity of the first order and the intensity of the zero-order. Our results allow the rapid design and characterization of self-focusing varied line-spaced gratings as well as optimal microstructures for targeted far-field diffraction patterns, which are playing key roles in spectroscopy and monochromatization applications.

Keywords: diffraction grating, neural network, optical structures design, self-focusing

1. Introduction

Diffraction grating is a fundamental optical component which can disperse and diffract the light into several different directions. It is primarily used for spectroscopy and monochromatization [1], and then extended its applications to physics, biology, astronomy et al. [2]. The new proposed diffractive devices with subwavelength structures, such as metasurface [3, 4], zone plate [5], photon sieve [6], benefiting from the development of the microelectronics fabrication techniques, have gained great success in manipulating the

amplitude, phase and polarization of the diffraction pattern, especially in visible range. The common issue is the expensive cost for the fabrication of their intrinsic subwavelength features. Therefore, the diffraction grating with sophisticated functionalities is still necessary for further investigation due to its larger feature size.

Varied line-spaced grating (VLS grating), whose period changes following a certain rule, can split and focus the incident beam simultaneously because each pitch of the varied line-spaced grating will diffract the incident beam at different angles with the same illumination wavelength [7, 8]. The functionality of VLS grating simultaneously splitting and focusing light is unmatched by other gratings. However, the realization of controllable and highly efficient self-focusing is still an ill-posed inverse problem. Traditional inverse design method of varied line-spaced grating was usually based on intuitive considerations, systematic fine-tuning (grid searching) or other traditional optimization method [9], which would cost expensively both computation resources and time. A small change of its target properties will require a recalculation and re-optimization of the model which will consume a huge number of resources. Therefore, it is necessary to develop a method being able to work inversely to reconstruct or design the VLS grating through the target diffraction pattern on the focal plane.

Recently, artificial intelligence, especially deep learning, is blooming in the scientific research supported by the rapidly increasing computing power, especially with the application of the graphic processing unit (GPU) [10, 11]. Application of deep learning algorithm in photonics device design has been demonstrated a powerful method[12-19] including the design of metamaterial [12, 13], core-shell structures [14], photonics crystal [15] and grating [20]. Though the success of the deep-learning method in photonics and optics, there is still very limited work focus on the information-enriched diffraction field of the photonics structure [18, 21-24]. The far-field diffraction pattern is always under-estimated since the lack of the non-propagating evanescent near-field components, even though far field diffraction is much more practical than the near field one for many applications. Very recently, a deep subwavelength topological microscopy method, which utilized the far-field diffraction field as the input of the deep neural network, was proposed and demonstrated with a deep subwavelength retrieval resolution of the dimers [23, 24]. However, this is only for the analysis of the variation of the diffraction field of simple dimer structure, the feasibility of neural network analyzing the diffraction field of more complex structures, such as a varied line-spaced grating, still needs a further investigation.

Here, we introduce a high efficiency self-focusing varied line-spaced grating designed by the deep learning algorithm based on the target far-field diffraction pattern. The grating has been numerically and experimentally demonstrated the peak intensity of 1st order being two orders of magnitude stronger than the 0th order intensity on the focus plane. Numerically, this method can effectively retrieve the design parameters of the grating with an average of 5% error. Our grating would be a promising high-efficiency diffractive device for spectrometer application even extending to shorter wavelength, such as EUV and X-ray wavelength.

2. Results and Discussion

It is known that the period of the varied line-spaced grating changes following a certain rule. Each pitch of the varied line-spaced grating can diffract the light at different angles under the illumination of same wavelength incident. This offers the grating a chance to be self-focusing. This character means that this type of unconventional grating can split and focus incident beam simultaneously (see Figure 1). By introducing the rules of the variation of the grating's line space, a focus point could be found in its far-field diffraction propagation field.

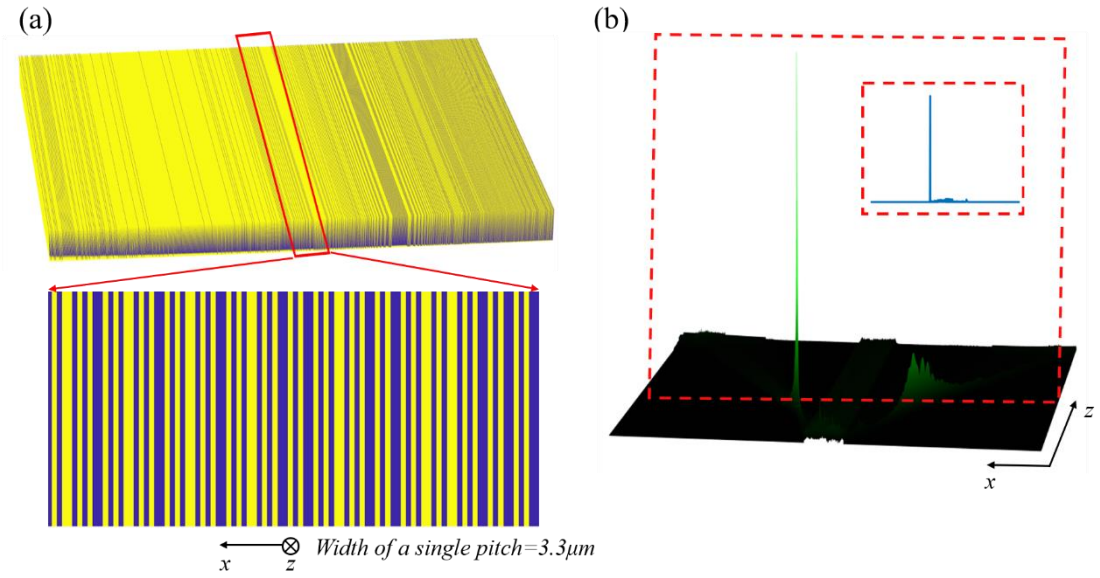

Fig. 1. (color online) A high efficiency varied period grating. (a) The sketch of varied period grating using the transmission function of Eq. (1). (b) Diffraction pattern of propagation intensity field map pattern of the grating design. Inset of (b) is the diffraction pattern on the focus plane of the varied period grating. The light propagates along the z positive axis.

Before applying algorithms to tackle the ill-posed inverse problem, controllable design of the high efficiency self-focusing VLS grating, we firstly introduce a representation of the grating. We use the transmission function as a representation of the 10 mm×10 mm VLS grating with 3001 grating grid units. We define that the duty cycle of transmission part of the

VLS grating is 50%, which can guarantee suppressing the even diffraction orders and increase the diffraction efficiency of 1st order. Utilizing the symmetry property of the cos function, we consider one-dimensional binary grating with the period variation of the variable grating period grating satisfying the following transmission function $t(x_i)$:

$$t(x_i) = \begin{cases} 1, & \frac{cos(2\pi x_i)}{T_{01}+Ax_i+Bx_i^2} > 0 \\ 0, & \frac{cos(2\pi x_i)}{T_{01}+Ax_i+Bx_i^2} \leq 0 \end{cases} \quad (1)$$

where T01 is the initial grating pitch, x_i is the i-th ($0 \leq i \leq 3000$) grid unit position (from 0 to 10 mm), and A, B are the coefficients of first and second order, respectively. Higher-order terms are not considered here and usually ignored due to its very little contribution on the change of the grating period.

Then, we introduce the deep convolutional neural network algorithm, as shown in Fig. 2, to assist us in reconstructing the VLS grating. Fig. 2(a) shows this fundamental picture of the physics. Diffraction intensity distribution on the focal plane obtained by the detector is used as the input of the deep convolutional neural network, and the parameters A, B, T01 of the grating transmission function as the output of the network. Deep convolutional neural network is selected because it can represent the diffraction pattern into higher dimensions through the convolution operation which is not available in the deep fully connected network. This will help the deep neural network understand the hidden information in a more sophisticated way.

To demonstrate this deep learning-assisted parameters reconstruction and grating inverse design method, we use a deep convolutional neural network consisting mainly 4 convolutional network layers and 2 fully connected layers (see Figure 2(b) for detailed hyperparameters)). The weights and bias of the convolutional kernel and fully connected neurons are optimized by the Stochastic Gradient Descent (SGD) with momentum optimization method. The performance of the regression network is evaluated using the Mean Squared Error (MSE) loss function activated by the sigmoid activation function of the output layer, and ReLU activation function of the other layers.

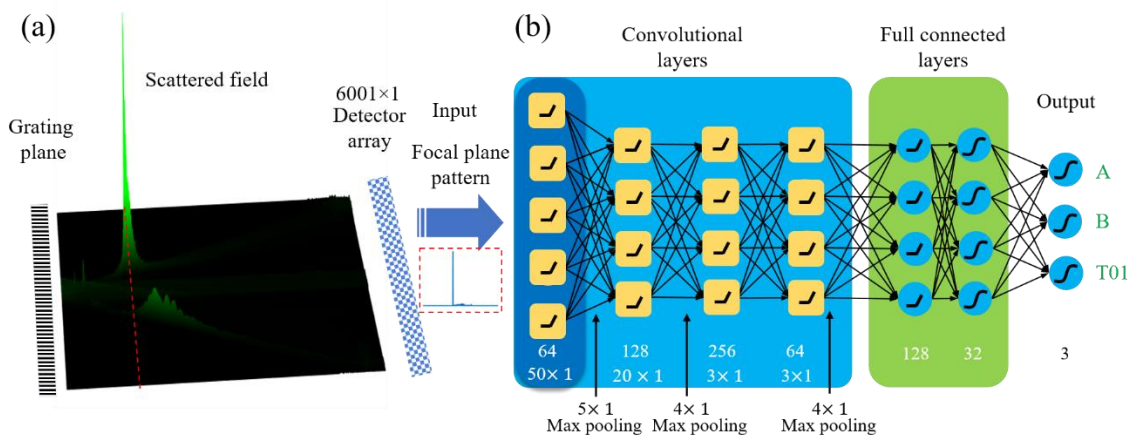

Fig. 2. (color online) Schematic of the deep-learning-based parameters retrieval and inverse design. (a) The scattering field of the grating on the focus plane is recorded by the detector array and transferred to neural network as input. (b) The deep convolutional neural network framework consists 4 convolutional layer and 2 full-connected layers. Here, yellow round squares and blue circles represent the convolutional neurons and fully connected neurons, respectively. The input is scattering pattern on focal plane and the output is the three parameters of the structure A, B, T_{01}.

Apart from a reasonable set of network hyperparameters, building a reliable, effective, and practical training dataset is also crucial for a trustable neural network[16, 25]. Here, we firstly generated the uniformly random parameters set with in the range $1\times10^{-5}<A<1\times10^{-2}$, $2\times10^{-9}<B<2\times10^{-6}$ and $1<T_{01}<6$. They will be regarded as the ground truth of the neural network and used for building the VLS grating design set. In order to limit the precision of the generated random number, we discretize each range of the parameters into 10,000 equally distributed numbers before the dataset generation. The calculation of the free space propagation field from the gratings is carried out using an in-house built Fourier angular spectrum solver. The diffraction pattern on the focal plane is extracted as the input of the neural network, because they are of our primary attention.

It shall note that our parameterized representation of the grating is qualitatively different from that designing with random generated pixelated designs, most of which are very far from optimal. It is known that the requirement of the size of the training dataset exponentially scales with the amount of the designing parameters. In our case, generating sufficient quantities of the grating design with 3001 pixels randomly would be practically difficult. Also, our deep learning algorithm is different from those feeding all designs in full parameters space ($(10^4)^3=10^{12}$ designs in our case) into the artificial neural networks. Because high first-order diffraction peak intensity I_1, low zero-order diffraction intensity I_0 is highly desired, we artificially selected the grating parameters with $I_1/I_0>2$ for our neural network training. The

dataset with only high-performance grating parameters being fed to the deep learning algorithms helps the neural network focusing on learning features harvested from the space of high-performance VLS grating designs, rather than attempting to extracting features from the designs far from optimal.

In these manners, the network is able to produce the high-performance designs of the grating diffracting desired pattern more effectively with substantially less training data. We generated N=20,000 sets of parameters of the grating transmission function, of which randomly distributed with 14,000 sets of data for training, 3,000 sets for validation, and the remaining 3,000 sets for testing the performance after training.

The results of our numerical retrieval of the parameters of the transmission function are presented in Figure 3. They demonstrate that the dimensions of parameters B and T_{01} can be retrieved accurately. The recovery rate of our neural network, calculated by Eq. (2), is 94.4%.

$$recoverR = 1 - \frac{1}{3N}\sum_{k=1}^{3}\sum_{m=1}^{N}\frac{|r_{k,i}-g_{k,m}|}{g_{k,m}} \quad (2)$$

Here, k represents three categorial of the parameters *A*, *B*, T_{01}, and *m* means the m^{th} testing sample. $p_{k,m}$ and $g_{k,m}$ means the predicted value and ground truth value of one test, respectively. Indeed, on Figure 3 the solid red, green, blue lines correspond to the median of the true values of the parameters as a function of the predicted values, whereas the black dash line is the bisector of the first quadrant representing perfect matching between true and predicted parameters. The performance of the neural network is quantified by the interquartile range (IQR), within which 50% of the true values are found. Since IQR does not vary significantly with the value of the parameters, we use its mean relative deviation to quantitively. The average IQRs of the retrieval of A, B and T_{01} are around 1.31×10^{-4}, 4.47×10^{-8}, 0.19, respectively.

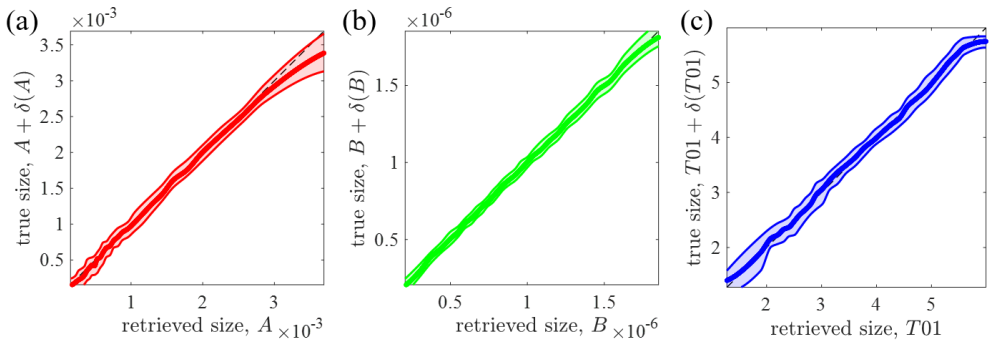

Fig. 3. (color online) The retrieval of the parameters of the VLS grating transmission function, A, B, T_{01}. (a-c) are the retrieval parameters distribution of A (red), B (green), T01 (blue), respectively. The spread means the IQR of the retrieved error distribution.

The numerical transmission function reconstruction performed with large training sets confirmed that artificial intelligence enabled retrieval of the target grating properties from the intensity patterns of the far-field diffraction. There are two factors contributing to this performance: (1) The deep neural network trained on a reasonable size of dataset creates an accurate and strong deconvolution mechanism. (2) Prior knowledge and sparsity of the representation of the grating transmission function advance the retrieval of the parameters, which is similar as that how sparsity boosts "blind" compressed sensing techniques [26].

Further, we used the trained deep convolutional neural network to recover the transmission function parameters of the VLS grating with higher first-order diffraction peak intensity by feeding a target diffraction pattern on the focal plane. As the orange line shown in Fig. 4 (a), we feed a diffraction pattern, whose first and zero order diffraction peak intensities are $I_1 = 1$ and $I_0 = 0.01$, respectively. We can obtain a set of parameters ($A=8.976\times10^{-5}$, $B=1.500\times10^{-8}$, $T_{01}=5.7575$) from the neural network, by which we can calculate the corresponding focal plane diffraction pattern shown by the blue line in the Fig. 4 (a). The first order focus is at 10 mm away from the grating. It shows that the diffraction pattern of produced by the designed grating has a good match with the target pattern, although we can see the differences in the zoom-in image. The difference of the first-order position relative deviation is only a negligible value of 0.5%. We also showed the propagation field of the designed grating in Fig. 4 (b). The diffraction intensity distribution meets our expectations.

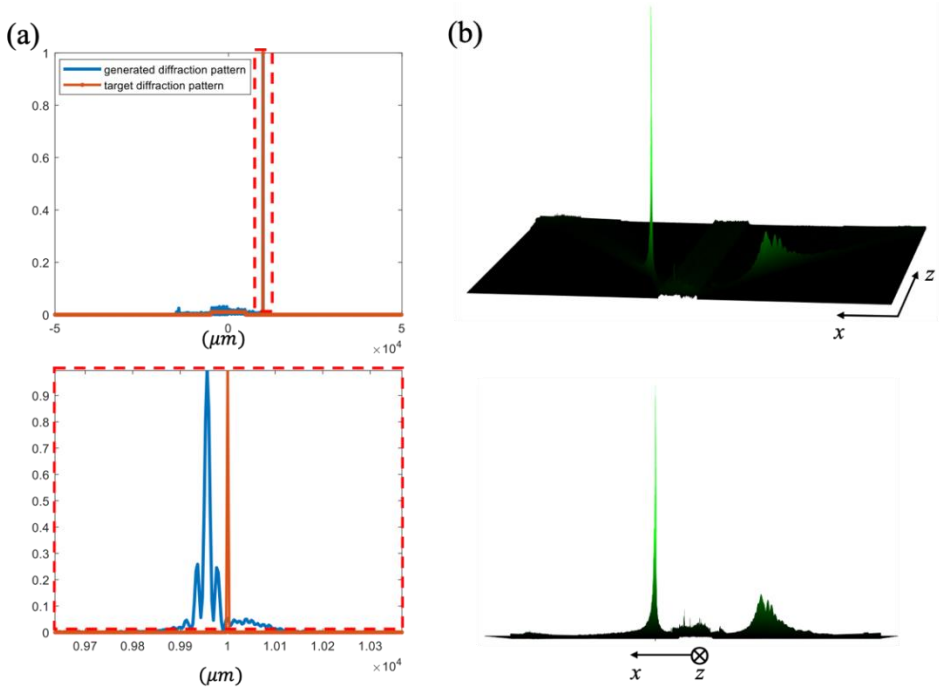

Fig. 4. (color online) Quantitative comparison between (a) Simulated and (b) target diffraction pattern. Red dash rectangle gives the zoom-in image around first order diffraction.

We have demonstrated numerically our VLS grating can split and focus the incident light. To verify the numerical prediction, we fabricated the 10 mm×10 mm VLS grating on the glass substrate. First, a 110nm chromium layer is deposited on the substrate using electron beam evaporation followed by spinning a layer of positive photo resist. Then, the grating design layout is transferred onto the resist layer by laser direct writing lithography. Next, after development, wet etching technique is used to transfer the pattern to the chromium layer. Finally, the VLS grating (see inset of Fig.5(a)) is obtained after removing the resist and cleaning.

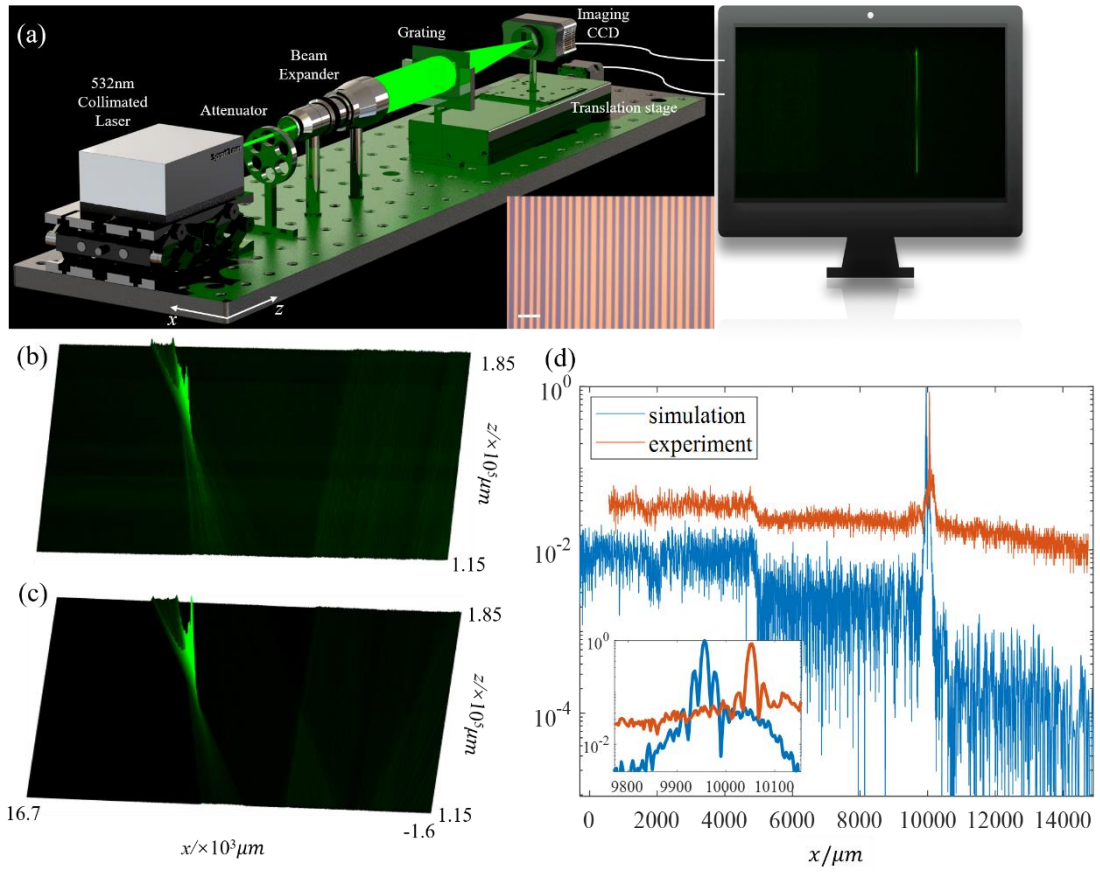

Fig. 5. (color online) Experimental demonstration of the high efficiency VLS grating. (a) Optical experiment setup using 532nm collimated laser illuminated on the laser after a beam expander. The diffraction pattern is collected by the CCD camera and pass through the computer. Inset: the physical VLS grating. Scale: 20μm. (b) Experimentally measured and (c) Numerical calculated propagating diffraction pattern around the focus plane(±3.5mm off the focus plane.). (d) Comparisons of the diffraction pattern on the focus plane between simulation and experiment. Inset: the profile near the first order.

The proof-of-principle experimental demonstration of the deep learning assisted design high efficiency VLS grating was carried out in a custom-built optical setup (see Fig. 5(a)). The coherent laser source at wavelength λ=532nm (Lighthouse Photonics Sprout-G 532nm, 1mW) is illuminated onto the grating after an attenuator and a beam expander. Here, the attenuator is to avoid the saturation of the detector and the beam expander is used for generating plane wave to make the illumination beam larger than the grating area. Therefore, the incident area is 10 mm×10 mm on the VLS grating as the same setting in our numerical simulation. The imaging detector is moved along z axis to get the diffraction pattern from -30mm to 30mm off the focus plane with a step of 1mm.

The diffraction pattern is collected by the Basler acA4112-30μm USB 3.0 Mono color camera (Sony IMX253 CMOS sensor, 30 frames per second at 12.3 MP Resolution). The pixel size is 3.45μm×3.45μm, assuming the number of pixels is 4096×3000, and the size of the CCD

photosensitive area is 14.11mm×10.3mm. An example of the detected raw image is shown in the computer screen of Fig. 5(a). The experimental propagating diffraction pattern of the fabricated physical self-focusing VLS grating, which is shown in Fig. 5(b), matches well qualitatively with that of the numerical calculated VLS grating (see Fig. 5(c)). A clear enhancement at the 1st order diffraction can be seen in the propagation field pattern for both cases. As also shown in the Fig. 5(d), the diffraction pattern on the focus plane also shows a good match quantitatively between simulation and experiment. The FWHM being around 20μm and I_1/I_0 being around 64 in the experimental measurement is very close to that in the simulation with FWHM and I_1/I_0 being 12μm and 86, respectively. We argue that this small mismatch is possibly from the fabrication error and laser beam quality. It shall note that our grating outperforms near a factor of 10 comparing with the varied line spaced grating designed by conventional optimization method [27, 28] whose I_1/I_0 is 7.

3. Conclusion

In conclusion, we have numerically and experimentally demonstrated a high efficiency varied line-spaced grating, which employs deep learning algorithms to design the parameters of its transmission function inspiring from a target scattering pattern. Our grating also shows an enhancement of the first order diffraction peak intensity over a factor of 30 compared with the incident intensity and a high ratio between first order diffraction peak intensity and zero order intensity over 60. We expect that much better gratings design shall be possible with two-dimension grating structures and more sophisticated deep learning method as they will offer more flexibilities with more degree of freedoms in design and possibilities to unveil the deeply hidden high-dimensional information in the diffraction pattern. Although so far, we demonstrate the concept in visible wavelength, it is promising when extending the applications to shorter wavelength, such as EUV and X-ray wavelength.

Funding. This work was supported by the National Key Research and Development Program of China (Grant No. 2017YFA0206002); National Natural Science Foundation of China (Grant Nos. U1832217, 61804169, and 61821091).

Acknowledgments. T. Pu thanks the valuable discussion with Dr. N. Papasimakis from University of Southampton, UK and acknowledges the financial support from Chinese Scholarship Council (CSC No.201804910540).

References:

1. T. K. Gaylord and M. G. Moharam, "Analysis and applications of optical diffraction by gratings," **Proceedings of the IEEE 73**, 894-937 (1985).

2. N. Bonod and J. Neauport, "Diffraction gratings: from principles to applications in high-intensity lasers," **Advances in Optics and Photonics 8**, 156-199 (2016).
3. D. M. Lin, P. Y. Fan, E. Hasman, and M. L. Brongersma, "Dielectric gradient metasurface optical elements," **Science 345**, 298-302 (2014).
4. G. X. Zheng, H. Muhlenbernd, M. Kenney, G. X. Li, T. Zentgraf, and S. Zhang, "Metasurface holograms reaching 80% efficiency," **Nature Nanotechnology 10**, 308-312 (2015).
5. E. Di Fabrizio, F. Romanato, M. Gentili, S. Cabrini, B. Kaulich, J. Susini, and R. Barrett, "High-efficiency multilevel zone plates for keV X-rays," **Nature 401**, 895-898 (1999).
6. L. Kipp, M. Skibowski, R. L. Johnson, R. Berndt, R. Adelung, S. Harm, and R. Seemann, "Sharper images by focusing soft X-rays with photon sieves," **Nature 414**, 184-188 (2001).
7. C. H. Michael, "Varied Line-Space Gratings: Past, Present And Future," in **Proc. SPIE**, (1986),
8. M. Fujisawa, A. Harasawa, A. Agui, M. Watanabe, A. Kakizaki, S. Shin, T. Ishii, T. Kita, T. Harada, Y. Saitoh, and S. Suga, "Varied line-spacing plane grating monochromator for undulator beamline," **Review of Scientific Instruments 67**, 345-349 (1996).
9. C. F. Xue, L. Xue, Y. Q. Wu, Y. Wang, S. M. Yang, and R. Z. Tai, "A variable fixed-focus constant optimization method for a variable-included-angle varied-line-spacing plane-grating monochromator," **Journal of Synchrotron Radiation 26**, 1192-1197 (2019).
10. Y. LeCun, Y. Bengio, and G. Hinton, "Deep learning," Nature 521, 436-444 (2015).
11. J. Schmidhuber, "Deep learning in neural networks: An overview," **Neural Networks 61**, 85-117 (2015).
12. W. Ma, F. Cheng, and Y. M. Liu, "Deep-Learning-Enabled On-Demand Design of Chiral Metamaterials," **ACS Nano 12**, 6326-6334 (2018).
13. W. Ma, F. Cheng, Y. H. Xu, Q. L. Wen, and Y. M. Liu, "Probabilistic Representation and Inverse Design of Metamaterials Based on a Deep Generative Model with Semi-Supervised Learning Strategy," **Advanced Materials 31**, 9 (2019).
14. J. Peurifoy, Y. Shen, L. Jing, Y. Yang, F. Cano-Renteria, B. G. DeLacy, J. D. Joannopoulos, M. Tegmark, and M. Soljačić, "Nanophotonic particle simulation and inverse design using artificial neural networks," **Science Advances 4**, eaar4206 (2018).

15. Z. C. Liu, D. Y. Zhu, L. Raju, and W. S. Cai, "Tackling Photonic Inverse Design with Machine Learning," **Advanced Science, 15** (2021).
16. J. Jiang, D. Sell, S. Hoyer, J. Hickey, J. Yang, and J. A. Fan, "Free-Form Diffractive Metagrating Design Based on Generative Adversarial Networks," **ACS Nano 13**, 8872-8878 (2019).
17. J. Jiang, M. Chen, and J. A. Fan, "Deep neural networks for the evaluation and design of photonic devices," **Nature Reviews Materials** (2020).
18. L. C. O. Tiong, J. Kim, S. S. Han, and D. Kim, "Identification of crystal symmetry from noisy diffraction patterns by a shape analysis and deep learning," **Npj Computational Materials 6**, 11 (2020).
19. W. Ma, Z. Liu, Z. A. Kudyshev, A. Boltasseva, W. Cai, and Y. Liu, "Deep learning for the design of photonic structures," **Nature Photonics 15**, 77-90 (2021).
20. S. Inampudi and H. Mosallaei, "Neural network based design of metagratings," **Applied Physics Letters 112**, 5 (2018).
21. A. N. Zaloga, V. V. Stanovov, O. E. Bezrukova, P. S. Dubinin, and I. S. Yakimov, "Crystal symmetry classification from powder X-ray diffraction patterns using a convolutional neural network," **Materials Today Communications 25**, 6 (2020).
22. Z. Ding, E. Pascal, and M. De Graef, "Indexing of electron back-scatter diffraction patterns using a convolutional neural network," **Acta Materialia 199**, 370-382 (2020).
23. T. Pu, J. Y. Ou, N. Papasimakis, and N. I. Zheludev, "Label-free deeply subwavelength optical microscopy," **Applied Physics Letters 116**, 4 (2020).
24. T. C. Pu, J. Y. Ou, V. Savinov, G. H. Yuan, N. Papasimakis, and N. I. Zheludev, "Unlabeled Far-Field Deeply Subwavelength Topological Microscopy (DSTM)," **Advanced Science 8**, 8 (2021).
25. G. V. Trunk, "A Problem of Dimensionality: A Simple Example," **IEEE Transactions on Pattern Analysis and Machine Intelligence PAMI-1**, 306-307 (1979).
26. S. Gleichman and Y. C. Eldar, "Blind Compressed Sensing," **IEEE Transactions on Information Theory 57**, 6958-6975 (2011).
27. F. Jin, S. Liu, X. Zhu, C. Xie, and M. Liu, "Design, fabrication and self-focusing properties of varied line-space grating " **Opto-Electronic Engineering 36**, 48-52 (2009).
28. F. Jin, X. Zhu, H. Li, J. Ma, C. Xie, and S. Liu, "Study on properties of 2000 lp/mm X-ray transmission varied line-space gratings," **Acta Optica Sinica 30**, 1857-1860 (2010).